Acta Materialia 109 (2016) 330–340

Contents lists available at ScienceDirect

Acta Materialia

journal homepage: www.elsevier.com/locate/actamat

Full length article

Shear band relaxation in a deformed bulk metallic glass

I. Binkowski [a], G.P. Shrivastav [b], J. Horbach [b], S.V. Divinski [a, c, *], G. Wilde [a, d]

[a] Institute of Materials Physics, University of Münster, Wilhelm-Klemm-Str. 10, 48149 Münster, Germany
[b] Institute of Theoretical Physics II, University of Düsseldorf, Universitätsstr. 1, 40225 Düsseldorf, Germany
[c] National University of Science and Technology "MISiS", 119049, Leninsky pr.4, Moscow, Russia
[d] Institute of Nanochemistry and Nanobiology, School of Environmental and Chemical Engineering, Shanghai University, Shanghai 200444, PR China

ARTICLE INFO

Article history:
Received 20 November 2015
Received in revised form
23 February 2016
Accepted 26 February 2016
Available online 11 March 2016

Keywords:
Bulk metallic glass
Shear transformation zone
Shear band
Diffusion
MD simulation

ABSTRACT

Relaxation of shear bands in a $Pd_{40}Ni_{40}P_{20}$ bulk metallic glass was investigated by radiotracer diffusion allowing to determine for the first time the effective activation enthalpy of diffusion along shear bands in a deformed glass. The shear bands relax during annealing below the glass transition temperature and the diffusion enhancement reveals unexpectedly a non-monotonous, cross-over behavior. The development of shear bands and the subsequent relaxation of stresses after the shear had been switched off are characterized on microscopic to mesoscopic length scales by molecular dynamics simulation subjecting a model glass to a constant strain rate. Mean-squared displacements as well as strain maps indicate that the heterogeneity, as manifested by shear bands in the systems under shear, persist after the shear was switched off. We observe a continued relaxation of residual stresses that remain localized in regions where the shear band has been present before, although the system is – different from the macroscopic experiment – homogeneous with respect to the local density. These results indicate that even on a local scale one may expect strong dynamic heterogeneity in deformed glassy solids due to shear banding that correlates with the existence of short-circuit type diffusion on a macroscale. The results thus suggest that plastically deformed metallic glasses present poly-amorphous systems that necessitate descriptions that are analogous to multiphase materials including the presence of heterophase interfaces.

1. Introduction

Although non-homogenous plastic deformation of bulk metallic glasses (BMGs) via the formation of shear bands attracted increased attention in the past [1,2], it is still far from being resolved, see e.g. the reviews in Refs. [3,4]. As a generally accepted concept, so-called "shear transformation zones" (STZ), i.e. areas in which groups of atoms collectively undergo a local shear transformation, have been introduced [5] as "unit carriers" of plastic deformation in metallic glasses. A cross-over from random 3-dimensional shear events (STZ formation) to correlated 2-dimensional dynamics has been brought forward to explain the observed shear banding in metallic glasses [6]. Although the activation of a single STZ event is not inevitably related to a change of the excess volume, shear bands are often described in terms of excess volume accumulation [3,7]. Recently, we investigated diffusion in deformed $Pd_{40}Ni_{40}P_{20}$ (at. %; in what follows we will use the abbreviation PdNiP) glass, in which almost a single family of shear bands was introduced, and were able to unambiguously prescribe the observed enormous enhancement of the diffusion rate to an ultra-fast atomic transport along these quasi-2-dimensional pathways [8]. The tracer concentrations in the corresponding concentration profiles, which were related to shear band diffusion, were shown to scale with the number density of the introduced shear bands (that in turn scales with the imposed strain), substantiating the reliability of the measurements. Nevertheless, dedicated TEM measurements revealed strong and probably characteristic changes of the specific volume along shear bands [9,10], with alternating regions of diluted and denser regions.

These results indicate significant modifications of the local structure of the glassy material inside the shear bands compared to the surrounding matrix, which have been revealed by local analyses via fluctuation electron microscopy [9,10], too. Additionally, these results point out that deformed glasses containing shear bands might be treated in analogy to a two-phase material including heterophase interfaces, with the second phase being the shear band phase that has undergone strong structural modifications due to the applied shear. Such structural modifications should also affect characteristic glass properties such as the relaxation dynamics and, potentially, might even affect the structure and properties of the matrix zones surrounding the shear bands via an

* Corresponding author.
E-mail address: divin@uni-muenster.de (S.V. Divinski).

http://dx.doi.org/10.1016/j.actamat.2016.02.061
1359-6454/

exchange of the excess volume. On the other hand, structural relaxation is a characteristic process of glasses and thus serves as a sensitive probe for analyzing the presence of such an apparent poly-amorphicity in deformed metallic glasses.

In order to address the relaxation behavior of shear bands, in the present paper the diffusion rates in plastically deformed PdNiP glasses are experimentally measured as function of temperature and varying annealing and pre-annealing times. These measurements target the relaxation behavior that is specific of the glassy material inside the shear bands only, which is not possible by macroscopically averaging measurements, since the fraction of matter inside the shear bands is only of the order of 10^{-4} to 10^{-3} in a moderately deformed glass. Such information is, however, vital in order to understand the modifications of the structure of the glass inside the shear bands, as well as the possible coupling of excess volume fluxes and excess volume re-distribution inside the shear bands and within the surrounding matrix.

Complementary to the experiments, shear band relaxation is investigated by molecular dynamics (MD) computer simulations of a simple model of $Ni_{80}P_{20}$, namely a binary glass-forming Lennard-Jones (LJ) mixture, sheared with a constant strain rate. A small shear rate is applied that is associated with the formation of a shear band. Subsequently, the stress relaxation was analyzed by switching off the shear at different strain values. As a matter of fact, the shear stress does not decay to zero after switching off the shear field, but it tends to approach a finite value in the long-time limit and thus the resulting glass structure, albeit not sheared anymore, is established to remain under stress. Different from the response in the supercooled liquid state [11], such residual stress has been found to be the generic case with respect to stress relaxation after switching-off of shear in glassy solids [12]. Furthermore, the residual stresses are found to be *heterogeneously* distributed in the glass sample, thus reflecting the memory of the shear band, as formed in the sheared system. We analyze the formation of shear bands by a methodology that we have recently developed in the context of a sheared soft-sphere mixture in its glass state [13,14]. To this end, maps of the local mean-squared displacements (MSDs) are computed. The simple LJ-type glass-forming system is deliberately chosen in the present case to investigate the generic features of strain localization upon deformation on a well-characterized glass. The results of this approach will be discussed in the context of analyzing the microscopic origin of the observed macroscopic diffusion data, particularly concerning the existence of short circuits for diffusion transport in deformed glasses, namely the shear bands.

The simulations show that on microscopic to mesoscopic length scales the shear bands do not lead to heterogeneities that can be characterized by a significant variation of the local density, as found experimentally on significantly larger scales [9,10]. However, residual stresses are spatially localized in the region where the shear band was created earlier and the simulation can disentangle how these localized residual stresses affect the mechanical properties of the glass. Moreover, the direct comparison between experimental results (which involve macroscopically averaged data) and simulations allows analyzing the unexpectedly complex relaxation behavior of shear bands in metallic glasses that needs to be taken into account for any constitutive description of the plastic response of metallic glasses.

2. Experimental and simulation details

2.1. Material and characterization

PdNiP-based bulk metallic glass with the composition of $Pd_{40}Ni_{40}P_{20}$ (in at.%) was prepared by direct melting of palladium (purity 99.95 %) and Ni_2P powder (purity 99.5 %) in an alumina crucible using an induction furnace in a purified argon atmosphere. The chemical compositions of the samples were confirmed by atomic absorption spectroscopy (Mikroanalytisches Labor Pascher, Germany). The crystalline master alloy was re-melted and then chill-cast into a copper mold with a $1 \times 10 \times 30$ mm^3 cavity.

A glassy sample was plastically deformed by cold rolling in one step at room temperature. The deformation degree, ε, was determined by the thickness reduction and the strain rate, $\dot{\varepsilon}$, was estimated at about 5.5 s^{-1}. Cold rolling of the glassy samples led to shear band formation, which was detected by optical microscopy of the shear offset on the specimens surfaces. Plastic deformation to a relatively low strain of about 8% was applied and the resulting shear band density, ρ_{SB}, was estimated at about 0.06 μm^{-1}.

X-ray diffraction was performed using a Siemens D-5000 diffractometer equipped with a Cu cathode, a K_α monochromator, and a rotating sample holder in the $\theta-2\theta$ geometry, using a point detector.

Differential scanning calorimetry (DSC) characterization was performed by a Perkin Elmer Diamond power compensated DSC applying a constant heating rate of 20 K/min in a temperature interval from 303 K to 798 K. The sample mass was about 20–30 mg. The measured signals on crystallized samples were used as baselines.

2.2. Radiotracer diffusion experiments

The ^{110m}Ag radioisotope (half-life of 252 days) with an initial specific activity of about 17 MBq/mg was produced by neutron irradiation of a natural silver chip at the research reactor FRM II, TU Munich, Germany. The activated chip was first dissolved in 20 μl of HNO_3 and dissolved in 20 ml of double-distilled water. A droplet of the highly diluted ^{110m}Ag solution was deposited onto the polished surface of each specimen and dried. The specimens were evacuated in silica ampoules to a residual pressure less than 10^{-4} Pa, sealed, and annealed. The annealing temperatures were chosen well below the calorimetric glass transition temperature. After the annealing treatments, the samples were reduced in diameter to remove the effect of lateral and/or surface diffusion.

The penetration profiles were determined by the serial sectioning technique using a precision parallel grinder. As a key point we mention that a second γ-isotope, ^{59}Fe, was further applied just before sectioning in order to check for the possible existence of micro-cracks (not seen by optical microscopy) and to guarantee the absence of any artifacts related to mechanical sectioning. The relative radioactivity of each section was measured with an intrinsic Ge γ-detector. The penetration profiles represent the plots of the measured relative specific radioactivity of the sections with subtracted background (which is proportional to the layer concentration of solute atoms) against the penetration depth, y, squared (according to the solution of the diffusion equation for the present boundary conditions). It was proven that the intensity of the ^{59}Fe isotope decreases below the detection limit already after several sections, thereby validating the reliability of the penetration profiles measured for ^{110m}Ag diffusion.

The relaxation behavior of shear bands at 498 K was investigated applying the radiotracer diffusion measurements as a sensitive probe of the shear band state. To this end, the diffusion sample, once annealed at 498 K for 3 days, was re-grinded and polished to background radioactivity, the ^{110m}Ag tracer was deposited again, and the diffusion annealing at 498 K was repeated for 3 more days. This step was repeated 3 times, so that the sample was finally annealed in total for 12 days. In parallel, DSC scans were performed after each heat treatment on a similar (non-radioactive) sample.

2.3. Atomistic model

We apply a model for $Ni_{80}P_{20}$ which has been proposed by Kob and Andersen [15]. It is a binary mixture of Lennard-Jones (LJ) particles (say A and B) with ratio 80:20. This mixture is an archetypical model for a glass former. Particles interact via the LJ potential which is defined as:

$$U_{\alpha\beta}^{LJ}(r) = \varphi_{\alpha\beta}(r) - \varphi_{\alpha\beta}(r_c) - (r - r_c)\frac{d\varphi_{\alpha\beta}}{dr}(r_c),$$
$$\varphi_{\alpha\beta}(r) = 4\varepsilon_{\alpha\beta}\left[\left(\frac{\sigma_{\alpha\beta}}{r}\right)^{12} - \left(\frac{\sigma_{\alpha\beta}}{r}\right)^{6}\right], \quad (1)$$

for $r < r_c = 2.5\sigma_{AA}$ and zero otherwise (with $\alpha,\beta = A, B$). The interaction among the particles is defined as $\varepsilon_{AA} = 1.0$, $\varepsilon_{AB} = 1.5\varepsilon_{AA}$ and $\varepsilon_{BB} = 0.5\varepsilon_{AA}$. The range of interactions is given as $\sigma_{AA} = 1.0$, $\sigma_{AB} = 0.8\sigma_{AA}$ and $\sigma_{AB} = 0.88\sigma_{AA}$. The masses of both particles are equal, i.e., $m_A = m_B = 1.0$. All quantities are expressed in LJ units in which the unit of length is σ_{AA}, energy is expressed in the units of ε_{AA}, and the unit of time is $m_{AA}\sigma_{AA}^2/\varepsilon_{AA}$ $(= \tau_{LJ})$.

We introduce an elongated box geometry with dimensions $L_x \times L_y \times L_z = 20\sigma_{AA} \times 20\sigma_{AA} \times 80\sigma_{AA}$ and density 1.2. We consider 30,720 A-type particles and 7680 B-type particles. The system is sheared at a constant shear rate using a simple planar Couette flow geometry, choosing x as the shear direction and y and z as the vorticity and gradient direction, respectively. Shear is imposed onto the system via Lees-Edwards boundary conditions [16] (modified periodic boundary conditions, where a particle that moves out of the simulation box in z direction is subject to a displacement in x direction according to the motion of the image cells below and above the simulation box with constant velocities $-U_{sx}$ and U_{sx}, respectively. With this scheme a linear velocity profile, $V_{s,x}(z) = \dot{\gamma}\left(z - \frac{L_z}{2}\right)$ (with $\dot{\gamma} = 2U_{s,x}/L_z$ the shear rate), is obtained in the steady state.

A schematic diagram of the simulation scheme is shown in Fig. 1. We consider first a binary LJ mixture equilibrated in the supercooled regime at a temperature of $T = 0.45$ and then quenched it instantaneously to a temperature $T = 0.2$, below the glass transition temperature (LJ units are used). After isothermal relaxation for $t = 10{,}000\tau_{LJ}$, we deformed the sample via pure shear with a constant strain rate $10^{-4}\sigma_{AA}/\tau_{LJ}$. The shear is switched off after deforming the sample up to 100% strain and it is allowed to relax until $t = 20{,}000\tau_{LJ}$. Shearing was used as the most reliable way to introduce a shear band in the simulation box.

The relaxation was further examined by switching off the shear at different strain values, ranging from 10 to 100%.

3. Results

3.1. Characterization of the amorphous state

The as-prepared samples were checked to be fully X-ray amorphous, Fig. 2a (black line), and the plastic deformation did not result in any detectable crystallization, Fig. 2a (blue line). Earlier investigations by TEM and also the observation of an increased low-temperature excess heat capacity (Boson peak) upon plastic deformation on the same glass have also confirmed the stability of the amorphous state of this alloy against deformation-induced crystal formation [17].

The measured DSC signals of as-quenched and deformed glasses are plotted in Fig. 2b. The glass transition temperature of the as-quenched glass was determined as 580 K (evaluated as the onset of the glass transition) in agreement with earlier reports [18] and it was almost not influenced by plastic deformation. The details on the effect of plastic deformation on the calorimetric characteristics of the PdNiP glass were analyzed in Ref. [19] in detail.

3.2. Radiotracer diffusion measurements

Four temperatures were chosen for the present study and the measured profiles are presented in Fig. 3. The parameters of diffusion annealing treatments are listed in Table 1. A deep penetration of the ^{110m}Ag tracer, to the depths of ten microns, is seen under conditions when bulk diffusion in the glassy matrix is completely frozen (the corresponding penetration depth is a small fraction of a nanometer). Note that the first several points of the penetration profiles are to be neglected due to grinding-in effects. However, the deep branches of the profiles are well resolved and reliable values of the pertinent diffusion coefficients can be determined.

The most deeply penetrating branches of the concentration profiles follow the Gaussian solution of the diffusion problem and the determined effective diffusion coefficients,

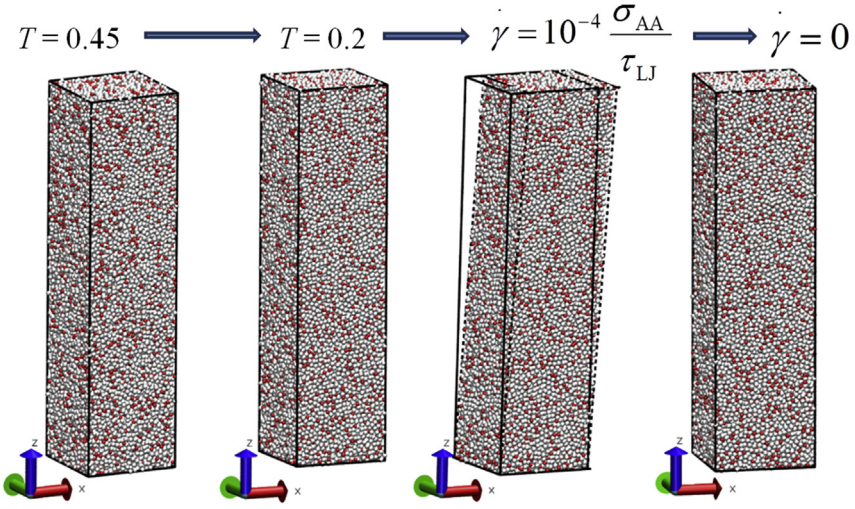

Fig. 1. Schematic diagram of shear-switch off simulation. Gray and red spheres represent Ni and P atoms in a model $Ni_{80}P_{20}$ system, respectively. Shear is applied in x direction, y and z correspond to the vorticity and gradient direction, respectively.

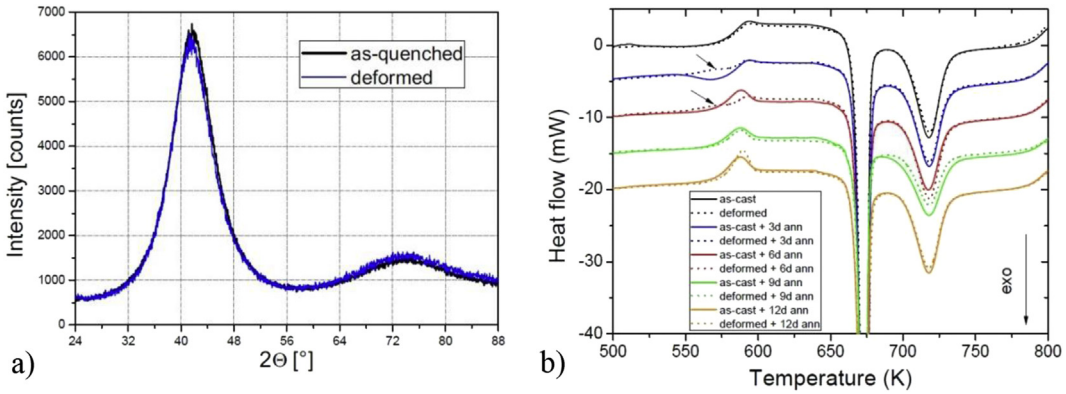

Fig. 2. X-ray diffraction of PdNiP glassy samples in as-quenched (black lines) and deformed (blue lines) states (a) and the corresponding DSC scans (b). In b) the DSC scans of as-quenched (solid lines) and deformed (dashed lines) samples after isothermal annealing treatments at 498 K for 3, 6, 9 and 12 days are shown, too. The arrows indicate additional peaks at the glass transition temperature observed for deformed samples. The DSC curves in b) are successively shifted along the Y-axis by −5 mW for a better visualization. (For interpretation of the references to colour in this figure legend, the reader is referred to the web version of this article).

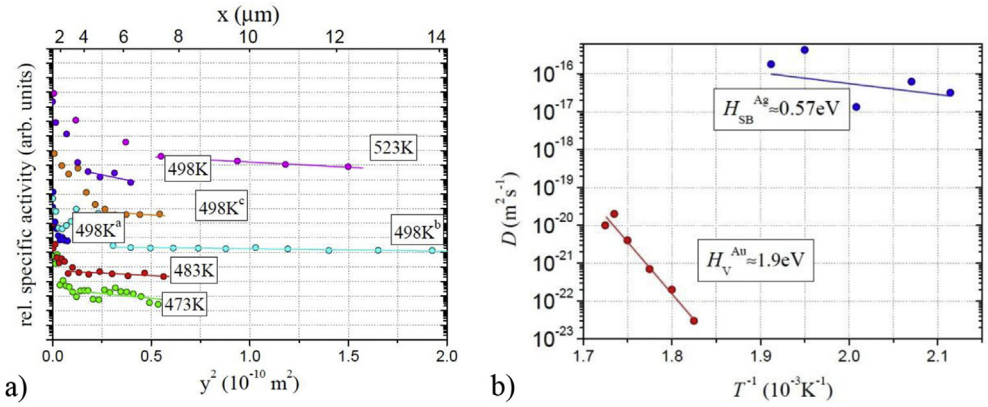

Fig. 3. Penetration profiles of ^{110m}Ag diffusion in deformed PdNiP glass (a) and the Arrhenius plot for ^{110m}Ag diffusion along shear bands (present work, blue symbols) in comparison to the diffusion coefficients measured for Au bulk diffusion [20] in PdNiP glass of nominally the same composition (red symbols) (b). In a), three profiles measured at 498 K, ^{a} – ^{c}, represent the effect of pre-annealing, see Table 1. (For interpretation of the references to colour in this figure legend, the reader is referred to the web version of this article).

Table 1
Temperatures and times of diffusion annealing treatments and the determined diffusion coefficients. The experimental uncertainty of the determined diffusion coefficients does not exceed 20%. The superscript-indexes ^{a}-^{c} are used to differentiate three different measurements at 498 K, see also Fig. 3a.

Temperature T (K)	Diffusion time t_{dif} (10^5 s)	Pre-annealing time t_{ann} (10^5 s)	Diff. coefficient D_{sb} (10^{-17} m^2/s)
473	2.59	0	3.16
483	2.59	0	6.18
498	2.59	0	1.33
523	2.59	0	11.8
498^{a}	2.59	2.59	24.6
498^{b}	2.59	5.18	4.75
498^{c}	2.59	7.78	1.52

$$D_{sb} = \frac{1}{4t}\left(-\frac{\partial \ln \bar{c}}{\partial y^2}\right)^{-1}, \quad (2)$$

are plotted in Fig. 3b as function of the inverse temperature.

Since radiotracer diffusion measurements were performed on glassy samples which may reveal a catastrophic failure (cracking) upon plastic deformation, the absence of interpenetrating internal porosity was checked. To this end, similarly to our previous study in Ref. [8], a liquid solution of a second tracer, ^{59}Fe, was dropped on the sample surface after diffusion annealing before sectioning. If open cracks would exist and surface diffusion would promote penetration of the ^{110m}Ag tracer, the second tracer would wet their surfaces, too, and thus would be detected at similar depths as the ^{110m}Ag tracer. This was definitely not the case and no signal from γ-decays of the ^{59}Fe radioisotope could be detected at depths larger than several micrometers. Such approach was previously used by us, e.g., to verify the existence of minute amounts (a few ppm) of interpenetrating (percolating) porosity in Cu subjected to severe plastic deformation [21].

Thus, the specific experimental set-up with application of two tracers and the dedicated TEM analyses did not reveal any open and percolating porosity in the deformed specimens, so that the diffusivities measured here represent solid-state diffusion through the shear bands.

3.3. Isothermal relaxation of shear bands

The relaxation behavior of shear bands at 498 K is investigated applying the radiotracer diffusion measurements as a sensitive probe of the shear band state. Unexpectedly, a non-monotonous time-dependence of the measured diffusion enhancement is found (Table 1 and Fig. 4a), with the diffusion rate along shear bands being first increasing and then decreasing at longer total annealing times.

Simultaneously, we followed structural changes of the glass by DSC and the characteristic changes of heat release at the glass transition temperature were recorded, Figs. 2b and 4b. As a result of plastic deformation, a second visible "peak" (indicated by arrows in Figs. 2b and 4b) at the glass transition, around 570 K, appears which is absent in the un-deformed state. The peak in the apparent specific heat that is directly proportional to the heat flow measured by DSC is directly related to the relaxation state of the glass [22] and it shows a distinct evolution with annealing time that is markedly different from the un-deformed state. After 3 days of annealing, the glass transition peak appears as two separate maxima of comparable, at least not strongly different magnitudes, see Fig. 4b, indicating the presence of two regions with different relaxational states (different fictive temperatures [23,24]).

We propose to characterize the deformation-induced changes of the glassy structures by the *difference* between the fictive temperatures [25] of deformed, T_f^{def}, and as-quenched, T_f^q, glasses, $\Delta T_f = T_f^{def} - T_f^q$. In Fig. 4a, this difference is plotted as a function of the annealing time and is compared to the measured annealing-time dependence of the shear band diffusion coefficient. Since the diffusion annealing time was 3 days in each experiment and since the shear band structure evolves further by relaxation during these heat treatments, the determined effective diffusion coefficients are plotted as bars spanning the time intervals of the given diffusion annealing.

Furthermore we have computed the difference between the fictive temperatures of pre-annealed, T_f^{p-e}, and as-quenched, T_f^q, glasses, $\Delta T_f = T_f^{p-e} - T_f^q$, and plotted it in Fig. 4a as a function of the annealing time. The pre-annealing has been performed at 498 K for 3 days.

3.4. Atomistic insights into shear band relaxation dynamics

To identify inhomogeneous flow patterns, information about the local mobility of particles in the system was quantified. We have employed two methods that turned out to be very efficient. First, we construct maps of local transverse displacements in gradient (z) direction that quantify non-affine motions caused by local structural rearrangements [13,14]. Secondly, maps of local mean-squared displacements in gradient (z) direction are computed, which were shown to reflect the macroscopic rheological response of the system on a single-particle level [26]. The coarse-grained MSD maps were used to identify the directed percolation transition marking the onset of the formation of shear bands [26]. These maps help to understand the atomistic nature of the observed non-monotonous relaxation behavior of diffusion acceleration inside shear bands.

In the MD simulation, the glass sample is first sheared applying a constant shear rate of $\dot{\gamma} = 10^{-4}$. As shown recently [27], at this shear rate a shear band forms at a strain of about 0.2, the width of which is growing diffusively with time. Thus, at a certain intermediate value of the strain the system exhibits an inhomogeneous flow pattern with non-flowing regions and regions of high mobility where the shear band is located. The central question that we address here is about the shear stress relaxation after the shear field has been switched off at a certain level of strain. We determine the shear stress as a function of time and analyze to what extent the inhomogeneous flow patterns, as formed in the sheared system, are reflected in a spatially inhomogeneous stress relaxation. Note that the stress is computed from the particle trajectories via the virial formula as in Ref. [11].

In Fig. 5a the stress relaxation is shown after the given levels of deformation. At all considered values of strain the stress remains first constant over about half an order of magnitude in time. This constant corresponds to the value of the stress that has been reached before the shear was switched off. After a transition time (which is shorter for higher imposed shear strains) the stress exhibits a smooth decrease that can be effectively described by a power law $\sigma \sim \tau^{-m}$, with the exponent m ranging from 1/8 (for low strains) to 1/5 (for 100% shear deformation). Eventually, one may expect that the stress approaches a constant non-zero value and thus as a final glass state subject to a finite residual stress is obtained.

To obtain information about spatial heterogeneities of the deformed samples with these residual stresses, we analyzed them in terms of maps of the mean-squared displacement and the non-affine strain, Figs. 5 and 6, respectively. Before the switching-off of the shear field, the MSD in the region where the shear band is located is much higher than in the rest of the system where the system has essentially not undergone the transition towards plastic flow, see Fig. 5b for the case of a sample with 100% shear deformation. In view of tracer diffusion data, one may expect that after the switching-off the mobility of particles is higher in regions where the shear band appeared before. To analyze this effect, we

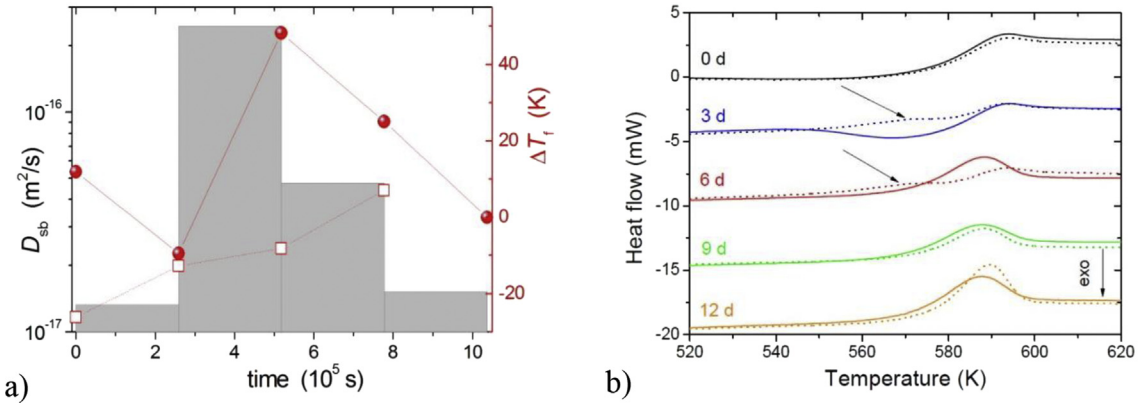

Fig. 4. The shear band diffusivity, D_{gb}, (gray bars, left ordinate), and the difference in the fictive temperatures, $\Delta T_f = T_f^{def} - T_f^q$, of deformed, T_f^{def}, and as-quenched, T_f^q, glasses (red spheres, right ordinate) as well as the difference in the fictive temperatures, $\Delta T_f = T_f^{p-e} - T_f^q$, of glasses pre-annealed at 498 K for 3 days, T_f^{p-e}, and as-quenched, T_f^q, (red squares, right ordinate) as functions of the total annealing time at 498 K (a) and the DSC scans of PdNiP glass in as-quenched (solid lines) and deformed (dashed lines) states without pre-annealing (black lines) and after isothermal annealing treatments at 498 K for 3 (blue), 6 (red), 9 (green) and 12 (magenta) days (b). Heat flow signals as measured near the glass transition temperature at about 580 K are shown (for full DSC scans see Fig. 2b). The DSC curves for different annealing times are successively shifted along the Y-axis by −5 mW for a better visualization. The arrows indicate extra peaks at glass transition temperature in deformed samples. (For interpretation of the references to colour in this figure legend, the reader is referred to the web version of this article).

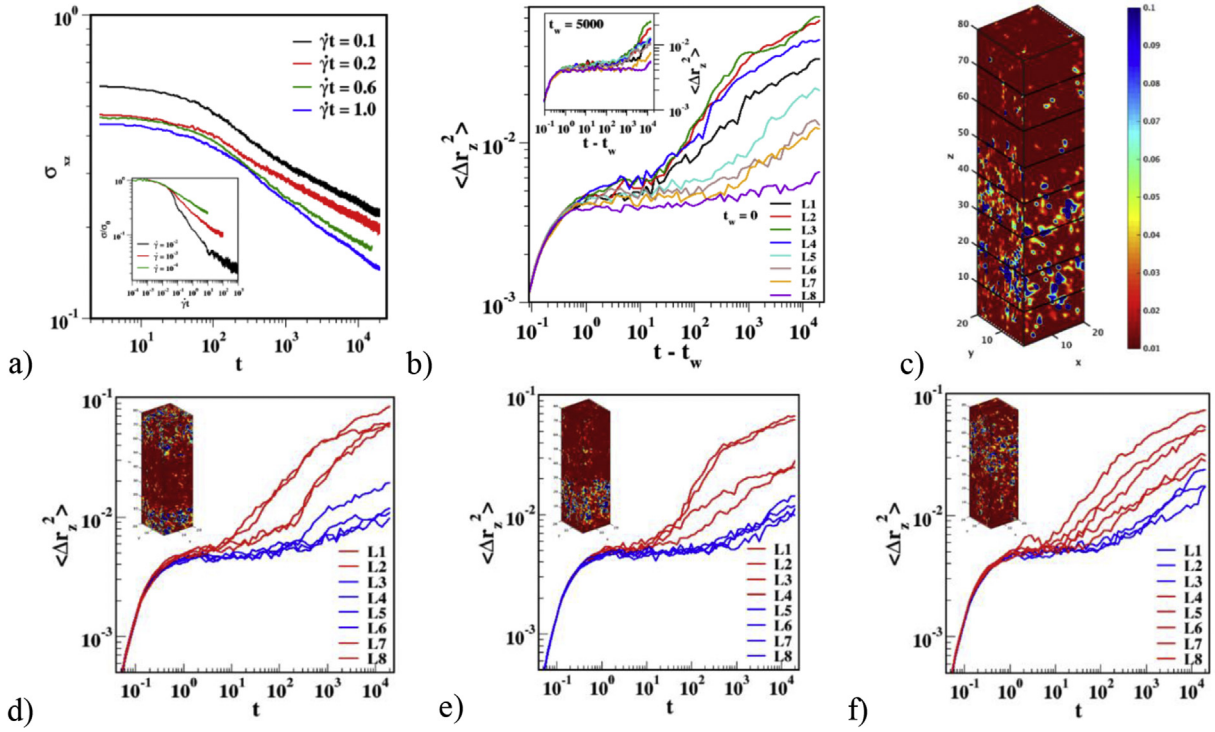

Fig. 5. Stress relaxation after 10%, 20%, 60% and 100% deformation for strain rate 10^{-4} with an inset showing the stress relaxation for strain rates 10^{-2}, 10^{-3}, 10^{-4} (a); layer-wise mean squared displacement (MSD) of particles during the stress relaxation after 100% deformation (b); snapshot of system divided into 8 layers of size $10\sigma_{AA}$ (c), and layer-wise MSDs for three different samples (d–f). The time origin in (b) is taken at the time when shear is switched off, $t_w = 0$ and the inset shows the MSD with time origin shifted at $t_w = 5000$. The color-coded lines correspond to the layers indicated in the snapshot. In (d–f) the layers in the shear band region are shown in red and layers outside shear band are shown in blue. (For interpretation of the references to colour in this figure legend, the reader is referred to the web version of this article).

decompose the system into 8 layers along the z direction (cf. illustration in Fig. 5d–f) and compute the average MSD in each of these layers. It is obvious that the MSDs in the shear band region are significantly higher than those in nearby layers (not affected by shear localization).

Recently, evidence has been given that there is a direct link between the macroscopic shear stress and the MSD, reflecting the response of the system to a shear field on a local level [26]. Therefore, one may expect that the behavior of MSD maps is directly linked to the residual stresses in the system; in particular, heterogeneities in the MSD may directly display an inhomogeneous distribution of residual stresses in the system. In Fig. 5b, the time where the shear field has been switched off, t_0, is chosen as the time origin for the MSD; the inset displays the corresponding curves for a time origin shifted by $t = 5000$ with respect to t_0. One can clearly infer from the figure that at positions where the shear band was located before the particles have still a much higher mobility. In the non-mobile regions, the MSD is essentially constant after the initial microscopic regime indicating the localization of the particles in the glass sample. The same behavior is also evident from the curves in the inset where the time origin is shifted with respect to t_0. Also in this case, the MSD increases with respect to the layers where the shear band was located.

Thus, a striking feature of the present simulation is that the diffusion enhancement is highly localized towards a shear band, as it is circumstantiated from the present macroscopic diffusion measurements. Moreover, the memory about the location of the shear band in the deformed sample is not only manifested in the MSD but also in terms of a localization of the non-affine strains in the system. This is indicated by MSD and strain maps that we show in Fig. 6 for the two times $t = 5000$ and $t = 10{,}000$ after the switch off of the shear field. In the shear-band region both the MSD and the strain are significantly higher than in the "inactive" part of the system. From this, it is also evident that the residual stresses are located in the region where the shear band was located before.

4. Discussion

The diffusion coefficients associated with Ag diffusion in shear bands follow an Arrhenius line and an effective activation enthalpy of about (55 ± 10) kJ/mol is determined from the corresponding slope, Fig. 3b. Since bulk diffusion of Ag in the PdNiP glass has not been measured yet, in Fig. 3b the shear band diffusivity of Ag atoms is compared to the diffusion coefficients of Au in nominally the same glass measured by Duine et al. [20]. One recognizes that the effective activation enthalpy of shear band diffusion, Q_{sb}, is about one third of that value for bulk diffusion in the glass matrix, Q_v, i.e. $Q_{sb}/Q_v \approx 55$ kJ mol^{-1}/182 kJ mol^{-1} ≈ 0.3. In crystalline solids such ratio would be characteristic for the relationship between the activation enthalpies of surface and bulk diffusion [28].

Shear banding is reported as a dominant mode of plastic deformation of granular media or rocks under certain conditions [29,30], though no data exist about the kinetics of atomic transport along such short-circuit paths. The present paper reveals for the first time that shear bands in a metallic glass present a path for enhanced diffusion with largely enhanced rates and remarkably low effective activation enthalpy, about 0.3 of that for bulk diffusion. This result appeals for proper investigations of transport phenomena in a broad range of natural materials which deform via shear band formation.

The nature of diffusion enhancement was investigated by isothermal measurements of the diffusion rate. A characteristic non-monotonic aging behavior is observed, Fig. 4a. Simultaneously, characteristic changes of the heat release near the glass transition

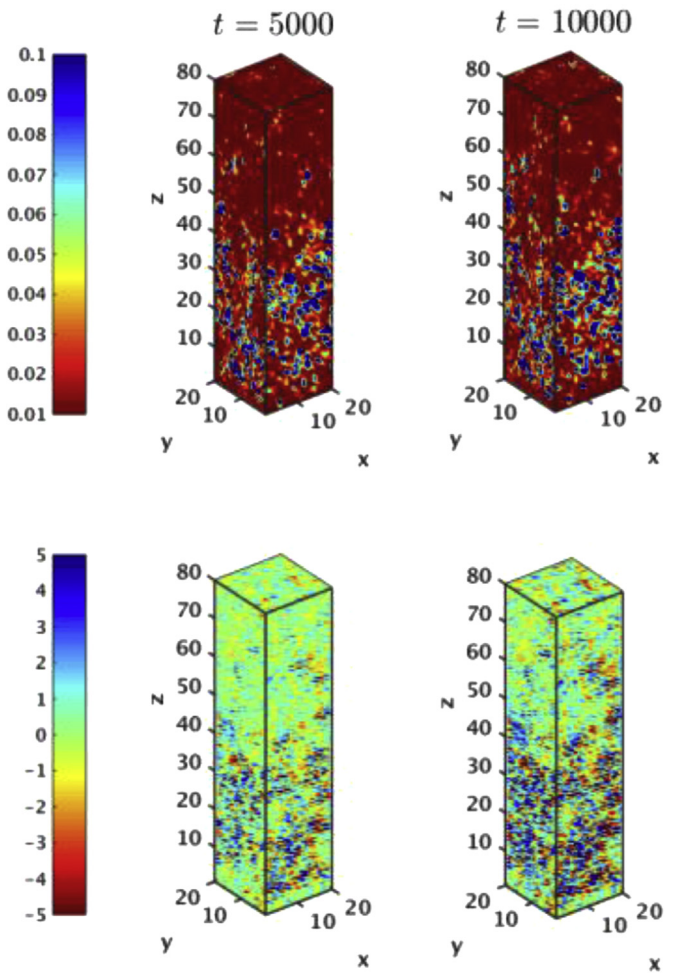

Fig. 6. MSD maps at $t = 5000$ and 10,000 (upper panels) and the corresponding strain maps (lower panels). Shear is switched off after 100% deformation.

temperature are seen, Fig. 4b. The plastic deformation is responsible for an additional "peak" at the glass transition which evolves with annealing at the temperature at which the relaxation behavior of shear band diffusion was analyzed, Fig. 4b. This behavior, especially the appearance of two separate maxima at T_g, indicates the presence of at least two regions with different excess volume content or basically different local configurations that occupy comparable volume fractions, since this signal is observed in a macroscopically averaging measurement. The last finding requires a special consideration. The volume fraction of glass inside of shear bands is estimated at about 10^{-3} from the measured density of shear bands, 0.06 μm^{-1}, and their typical thickness of about 10 nm. Thus, it is not just glass material inside of shear bands which attain new properties and contribute to a separate maximum at T_g. Yet, it is safe to consider that upon cold rolling the glass structure is modified in extended regions where not all of them result in shear bands. This view is supported by MD simulations which document that a signature of plastic deformation, i.e. residual stresses after shearing is switched-off, being especially manifested at shear bands, are heterogeneously distributed in the deformed matrix. Moreover, modifications of the glass structure on a micrometer scale around shear bands – a wide soft zone – were reported in nanoindentation experiments [31] and distinct changes of the glassy matrix related to the appearance of first STZs were concluded from amplitude dependent internal friction far below the onset of shear banding [19].

For a Pd–Ni–P glass of slightly different composition, similar modifications of the glass transition signal have been observed as a function of thermal annealing in the temperature interval of the glass transition [32]. Those modifications of the glass transition signal, that were found to be reversible, but with a significant hysteresis between formation and annihilation temperatures, have been shown to be correlated with modifications of the medium range order. The present findings correlate also with the existence of a broad spectrum of atomic-packing motifs in a bulk metallic glass upon deformation, as recently reported in Ref. [33] and the basically different relaxation of boson peaks in deformed glasses with respect to the undeformed state [17,34], which also indicates strongly that deformation can adjust new local medium range order motifs that, in the view of energy landscapes, might present local minima within a different metabasin. The fact that qualitatively similar observations were obtained for two different glasses (Pd-based [17] or Zr- based [34]) that had been subjected to different types and amounts of strain substantiates the general nature of these findings.

Upon continued annealing, the splitting of the peak vanishes, indicating that the majority of the volume of the specimen is in a similar relaxational state again, however fundamentally different from that of the un-deformed glass which does not reveal such a peak, Fig. 4b. After 6 days of annealing, the peak at the glass transition is most pronounced and decreases again in height with further annealing. Such complex time dependence of the relaxation peak at the glass transition is indicative of so-called "crossover" behavior [35,36], where the time scale of the annealing treatment and the time scales for excess volume re-distribution and annihilation compete.

The difference between fictive temperatures of as-quenched and deformed glasses as function of time at isothermal annealing, Fig. 4a, shows a generally unexpected and striking feature, it is first increased and then decreased and the annealing time dependence of the shear band diffusivity is very similar. In a simple free-volume picture, this observation is in agreement with the annealing-time evolution of the relaxation peak at the glass transition: the corresponding enthalpy is maximum when the relaxational state has acquired the highest amount of excess volume (corresponding to the highest peak maximum at the glass transition). Fig. 4a shows an example of a cross-over behavior observed for shear band diffusion and the fictive temperature excess related to the shear localization, both of them are occurring almost 100 K below the glass transition temperature. Previously, such a cross-over has been observed, e.g., for Young's modulus [37], Curie temperature [38], or viscosity [36] of metallic glasses far from the glass transition. The distinct feature is that in the present study a metallic glass has undergone plastic deformation at room temperature instead of thermal annealing below the glass transition as it was done in previous investigations concerning the cross-over behavior.

The specific aging behavior of metallic glasses and especially its rejuvenation as a function of thermal annealing schedules alone have been interpreted as being driven by atomic-scale internal stresses, local non-affine deformation, and inherent heterogeneity at the atomic scale [39,40]. The present results on deformed glass samples are in line with this view. However, the marked difference between the calorimetric responses around the glass transition of deformed and undeformed samples that experienced an identical thermal history supports the view that at similar excess energy increments, deformation is more effective in modifying the energy landscape of the material, giving rise to specific dynamics of glass relaxation.

In Fig. 4a the effects of room temperature plastic deformation (rolling) and pre-annealing at 498 K for 3 days on the annealing dependence of ΔT_f are compared and fundamentally different

evolutions are observed. While plastic deformation increases the fictive temperature ($\Delta T_f > 0$) and reveals a crossover-type behavior of ΔT_f with a distinct maximum, pre-annealing of the as-quenched glass decreases the fictive temperature ($\Delta T_f < 0$) and subsequently a monotonic aging behavior, $\Delta T_f \rightarrow 0$, is seen. These opposite trends lead us to conclude that the mechanical "activation" is a different approach to probe and alter the energy landscape of glassy materials and it cannot fully be described as similar to thermal annealing at some "effective temperature". This conclusion is strongly supported by the data on the Boson-peak behavior of as-quenched and deformed glasses after annealing treatments [17].

4.1. Phenomenological model for diffusion enhancement in shear bands

In what follows, a phenomenological model for the diffusion enhancement in shear bands is proposed that is able to account for the measured annealing-time dependence of the shear band diffusivity, annealing behavior of the calorimetric response on deformation, and the time dependence of MSD maps after switching off shearing in atomistic simulations.

We may suggest that the deformation of a BMG starts with the generation of STZs, black curve in Fig. 7a. The deformation level ε_1 corresponds to a regime that is still within the macroscopically 'elastic' regime of deformation. These STZs correspond to local shear events of groups of atoms and are probably not related to changes of the excess volume, Fig. 7b. A stochastic analysis of deformation in this regime reveals 3-dimensional generation (activation) of STZs, thus throughout the entire volume of the deformed glass [6].

At larger deformation, $\varepsilon = \varepsilon_2$, a transient regime begins. The formation of STZs becomes heterogeneous (red curve in Fig. 7a), and local shear events interact. The intersection of STZs could increase locally the excess volume (densifying the neighboring areas), Fig. 7b. These processes could be assumed to be accompanied by a redistribution of excess volume and the excess volume is accumulated at these locations ('shear band precursors').

At even higher deformation, $\varepsilon = \varepsilon_3$, the avalanche dynamics of STZs becomes clearly 2-dimensional, residual stresses are highly localized as it is seen in atomistic simulation, and shear bands appear, blue curve in Fig. 7a. This re-organization is accompanied by a net flow of the excess volume to the shear band, still one may assume that some fraction of the excess volume is retained nearby (in "shear band-affected" zones), Fig. 7b. This scenario agrees well with measurements of the indentation hardness [31,41] that found a soft zone adjacent to shear bands. In fact, this scenario also agrees with the observation that no strain was imparted except directly at shear bands [42], since an enhancement of the content of excess volume could proceed without macroscopically measurable strain.

Since in the proposed scenario a shear band is initiated as an avalanche-like self-organization of STZs along a given quasi-2-dimensional path, one may expect that there is no total flux of excess volume from the outside; excess volume just redistributes along the shear band. Still, one may expect that at later stages of the shear band propagation some additional excess volume may migrate in from the outside (where a surface step is formed). This idea is in agreement with enhanced diffusion along a SB, see Ref. [8] and the present data, but apparently contradicts to the STEM data [9,10] that local denser areas are alternatively observed, too. Yet, such alternating dilatation/densification [9,10] might be associated with a local topology of the shear band (which is not a plane) and the related in-plane compressive and tensile regions along the shear band path during propagation in a stick-slip manner [42], i.e. such regions might form at a later stage after the shear band has already been fully developed and serves as a slip "plane" with local deviations from the direction of maximum stress that act as local barriers for slip. Measurements of the local strain distribution along individual shear bands support this view [42]. Thus, we cannot omit the hypothesis of excess volume migration into the shear band if we assume that this additional excess volume contributes to some 'delamination'-like events between the shear band and the surrounding matrix, leaving denser portions of the shear band unchanged with the concomitant formation of the above described 'interfaces' between the shear band and the matrix. In fact, the recent observation of void formation localized within shear bands during late stages [41] fully agrees with this interpretation.

Accounting for this model of shear band initiation, one arrives at the existence of two additional relaxation processes in deformed glasses, namely inside the shear bands and in the deformation-activated matrix. Indications for the latter were gained via detailed analyses of the Boson peak relaxation in deformed glasses [17], too. Now, we have to take into account that thermally induced migration of excess volume in amorphous material, akin a delocalized vacancy in a crystalline material, might be kinetically more enhanced with respect to diffusion hops of tracer atoms. Having in mind a collective mechanism of diffusion in glassy solid, e.g. as a coupled motion of a string of atoms [43], we arrive at following scenario: Annealing below the glass transition temperature induces first a redistribution of excess volume in the shear bands and the surrounding matrix that increases the excess volume content in the

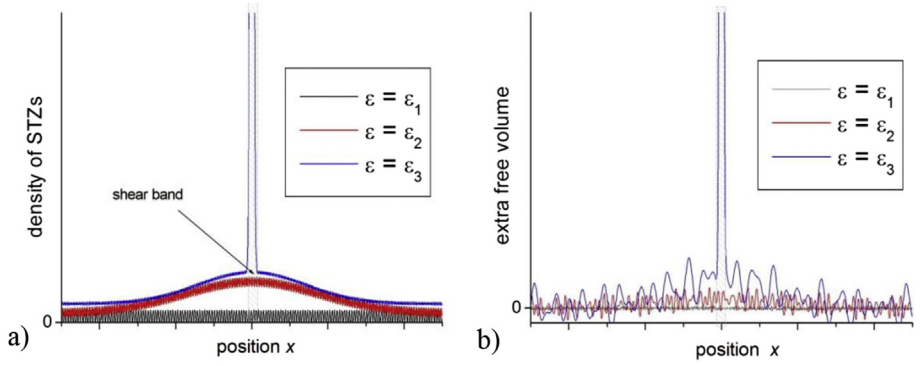

Fig. 7. Schematic evolution of the density of STZs (a) and that of the extra excess volume (b) as function of the strain ε. At low strains (in the macroscopically elastic region), $\varepsilon = \varepsilon_1$, there is a macroscopically homogeneous generation of STZs and the excess volume practically does not change, i.e. the additional excess volume is almost zero (black lines). If the strain increases, $\varepsilon = \varepsilon_2$ (transient regime), STZs begin to be activated/form inhomogeneously and dilute and denser local regions appear (red lines). At a higher strain (onset of plasticity), $\varepsilon = \varepsilon_3$, STZs self-organize in a shear band (marked by the shaded area) at some location and areas with additional excess volume appear (blue lines). (For interpretation of the references to colour in this figure legend, the reader is referred to the web version of this article).

shear bands and in fact enhances tracer diffusion along the shear band. Further relaxation of the excess volume proceeds mainly via transport along shear bands and the corresponding diffusion enhancement in shear bands decreases. This is exactly what is seen experimentally.

The atomistic simulations provide further hints towards this interpretation since the stress relaxation in the deformed glass occurs highly heterogeneously and residual stresses are associated with the formed shear band. Detailed analyses of MSD maps reveal that atomic mobility (which is related to the mean-squared displacement) in the deformed glass approaches first a plateau and then enhances further, exclusively in the layers closely related to the shear band, Fig. 5. These facts, although gained on different time and length scales, substantiate a non-monotonous and strongly heterogeneous relaxation behavior of deformed glasses. Moreover, this behavior seems to represent a generic feature of a glass-forming system and it does not necessarily include (although does not exclude, too) local chemical modifications related to shear banding.

According to a mesoscopic strain analysis [42], the propagation of individual shear bands occurs in a stick-slip manner of segments of the shear bands, accompanied with the formation of alternating dilated and densified segments of the single individual shear band. In the latter case the additional excess volume appears most probably as thin layers between the shear band and the matrix. The existence of such 'interfaces' (akin grain boundaries in crystalline materials) can be anticipated from diffusion measurements in which tracer propagation over at least 10 microns is recorded whereas dilute and dense regions of a given shear band alternate on a scale of 100–200 nm. In addition, the existence of such interfaces is also in agreement with the mechanical integrity of metallic glass specimens containing shear bands [8]. Note that two different zones of shear bands were reported in Ref. [7] and supported by nano-indentation tests in Ref. [40]. We suggest that these “interfaces” between two glassy states (matrix and deformation-transformed shear band) are responsible for the diffusion enhancement.

4.2. Heterogeneity of relaxation behavior of the deformed glass

Atomistic simulation substantiates that the residual stress is frozen in the deformed glass and remains highly localized to shear bands which promoted the imposed plastic deformation. The structure and kinetic heterogeneity is revealed on different levels, starting from the atomistic one (MSD and non-affine strain maps), mesoscopic (stick-slip behavior as found on a sub-micrometer scale using Digital Image Correlation analysis [42]) and the macroscopic level (the present results on tracer diffusion).

The time dependence of the MSD maps indicates different regimes, with a distinct change at longer times, revealing the occurrence of a two-stage process that in fact corresponds to a cross-over behavior. Analyzing the spatial correlations with the measured time dependence of the MSD showed that the second process, yielding the increase of the MSD at longer times, is presumably associated with active centers in the spatial region that was formerly forming the interface between shear band and matrix during shear. Even though the time scales between experiment and simulation are not comparable, this observation is in excellent agreement with the conclusions drawn from radiotracer diffusion experiments [8] that gave rise to postulating the presence of interface-like states that could act as fast diffusion pathways, independent of the presence of dilated or densified regions along a given shear band. The fact that an enhanced MSD was observed long after the shear stress had been turned off substantiates the occurrence of a structural modification of the shear band regions serving to enhance mobility.

It is important that the present MD results are of general nature; in fact we deliberately made a point *not* to try mimicing a particular material or its interaction potentials, but to analyze the behavior of a well-characterized system. A variation of short- or medium-range order may cause the appearance of secondary peaks at T_g, as it can be deduced from DSC measurements on a slightly different PdNiP glass [32]. However, the slight changes in local composition can be equivalent to (or at least can accompany) a re-organization of local excess volume and the related building-up of local residual stresses. In both cases, locally, two different glassy structures would result that would be heterogeneously distributed in the material. According to the present MD simulations, persistent local residual stresses on an atomic scale are a direct signature of the deformation localization in a metallic glass and they are present even in absence of chemical heterogeneities. The distribution of these stresses correlates to the MSD map which highlights enhanced kinetics in shear bands. These findings do independently support the experimental observation of a short-circuit-type of diffusion enhancement in deformed glass and suggest its general nature.

Though an increase of the local excess volume was not explicitly found in MD simulation on accessible length scales, we assume that it is the excess volume accumulation which promotes enhanced diffusion that is observed on a macro-scale. The generation of the excess volume might be inherently related to the stick-slip mode of plastic deformation [42] and an average dilatation related to a shear band (with alternating dense/dilute regions on a 100 nm scale) was unambiguously determined in dedicated TEM measurements [9,10].

It is important to note that the existence of alternating denser and diluted regions provides conditions for mechanical (meta-) stability of the localized (extra) excess volume against macroscopic displacements of the matrix as a whole, as soon as diffusion events are frozen.

4.3. Diffusion enhancement in a shear band

Adapting the volume-fluctuation model [44,45] that has originally been developed for polycrystalline solids, the diffusion coefficient D_{sb} of shear bands (in analogy to the diffusivity of grain boundaries) may be described as:

$$D_{sb} = D_v \exp\left(\frac{K_{sb}\Delta v_{sb}}{2k_B T}\right) \tag{3}$$

where D_v is the bulk diffusion coefficient of the glass in the relaxed state, K_{sb} is the bulk compressibility of the shear band, Δv_{gb} is the deformation-induced excess volume per atom within the shear band, and k_B is Boltzmann's constant. The bulk compressibility of a shear band, K_{sb}, can be expressed as $K_{sb} = 2G_{sb}(1+\nu)/3(1-2\nu)$, where G_{sb} is the shear modulus of the shear band and ν denotes Poisson's ratio. According to our direct measurements, only small changes of the elastic moduli and of Poisson's ratio were found in the deformed glass [46]. As a first-order approximation, we assume that the shear modulus of the shear band is similar to that of matrix.

The average additional excess volume of a shear band in PdNiP can be estimated as 0.4%, although local values can approach even 9% [10]. Still, if we assume the formation of 'interfaces' between matrix and shear band, local values of Δv_{gb} can safely be estimated as 0.1Ω, where Ω is the atomic volume, taken here as 10^{-29} m^3. Inserting this value into Eq. (2), assuming $G_{sb} = 50$ GPa and using $\nu = 0.4$ for PdNiP [46], the ratio D_{sb}/D_v is about $6\cdot10^7$ at $T = 473$ K. Thus, Eq. (2) can reproduce the measured diffusion enhancement in shear bands over 7 to 8 orders of magnitude.

Now, relaxation behavior of the diffusion coefficient of a shear

band shall be analyzed. In the framework of the present model, it is the evolution of shear band compressibility K_{sb} and that of the excess volume Δv_{gb} which have to be evaluated.

Thermal annealing results in a non-monotonous evolution of the shear band diffusion coefficient. The behavior may be explained in a way similar to the idea of non-linear segregation suggested for the non-monotonous evolution of impurities at grain boundaries in crystalline materials [47,48]. We suggest that there is first a re-organization of the additional excess volume in shear bands with a given time constant constrained by mechanical equilibrium induced by mechanical deformation, i.e. by the formed densified/diluted regions. This reorganization is accompanied by extra excess volume flow from neighboring matrix areas. As a result there is a further increase of the excess volume localized at shear bands and consequently diffusion enhances. According to Eq. (2), a 10% increase of the local excess volume would be sufficient. Further annealing results in relaxation of the accumulated excess volume and the disappearance of the dense/dilute contrast in SBs, which would also allow the glassy material inside the shear band to re-organize such that the highest-mobility pathways are annihilated, resulting in a decrease of the shear band diffusivity as observed in the experiments. This empirical model is fully in line with the observed cross-over behavior, since the characteristic time scales for the initial re-organization/re-distribution of excess volume and the relaxation of the accumulated excess volume inside the shear bands are expected to be different. Thus, the present findings indicate a *correlation* between the diffusion rate along the shear bands and the time-evolution of the deformed glassy structures as revealed by DSC. In fact this correlation is not trivial, since, as mentioned above, the volume fraction of shear bands and that of the structure components visible in DSC experiments are strongly different. We suggest that the annealing treatment modifies the local glassy structures and presumably induces an extra flux of excess volume towards shear bands that affects the corresponding diffusion rates. The annealing-affected relaxation of local heterogeneities, which were formed due to deformation localization and were revealed by DSC, correlates with that of the kinetics of atomic transport along shear bands, probably along shear band-matrix 'interfaces', Fig. 4a. Tracer diffusion probes a state of these 'interfaces' and indicates the occurrence of local modifications along the diffusion path as a result of annealing, though these particular modifications are not visible for DSC, which presents a macroscopically averaging measurement method.

It is not only plastic deformation which modifies the local structure. Chemistry and the excess volume content of shear bands also trigger them into a different glassy state (without inducing nano-crystallization), but post-deformation relaxation imposes excess volume redistribution and the appearance of built-in residual stresses which affect the glass structure in terms of its corresponding potential energy landscape, thereby enabling the glass to trace new minima in the energy landscape. This behavior correlates with the fact that annealing does not erase the memory of a glass concerning the previous plastic deformation, which was found to persist even up to the crystallization temperature [19]. The present findings suggest a possibility of a further optimization of glass properties via combining deformation and heat treatments below the glass transition temperature. When we compare the energy input by thermal annealing and by small strain, we might not expect them to be very different. Yet, considerable changes were observed, with the deformation being more efficient to alter the state and the further evolution/relaxation of the glass. This may be due to the "directionality" or due to the fact that deformation addresses the "right" sites (the ones that are most susceptible for shear, which might also be related to the Boson peak). That might also be an issue concerning discussing the coupling of the Boson peak with the local structures and the energy landscape [19]. Moreover, time dependent stress relaxation along shear bands has recently been observed and a shear-band cavitation on micron scale has been reported [41]. Formation of cavities might be a fingerprint of excess volume localization in addition to local tensile stresses, the existence of which was pointed out in Ref. [41].

The involved inherent relaxation dynamics of the shear band structure has a further consequence on the measured activation value of shear band diffusion; in fact the latter has to be treated with caution as an effective value, which is still characteristic for kinetic processes with the corresponding relaxation times.

5. Summary

We have shown that atomic diffusivity in shear bands is enhanced by 7–8 orders of magnitude with respect to the glassy matrix. The effective activation enthalpy of shear band diffusion is found to be about one-third of the corresponding value for diffusion in the glassy bulk (the undeformed matrix). Moreover, atomistic simulation supports directly the view that the zones of enhanced mobility (the short circuit diffusion paths) are localized at "interfaces" between shear bands and the glass matrix indicating an inherent inhomogeneity of the excess volume distribution upon deformation.

The relaxation kinetics of diffusion enhancement along shear bands is measured for the first time and an unexpected, strongly non-monotonous behaviour is found – the effective diffusion coefficient increases first and then decreases. These changes are going in line with the appearance of a distinct calorimetric "peak" at the glass transition temperature upon relaxation after deformation and a characteristic development of the corresponding fictive temperature, both being attributed to inhomogeneous relaxation within the deformed glass. Moreover, a strong increase of the mean-squared displacement of atoms localized at a shear band is observed as a result of relaxation, substantiating that the evolution of the kinetics of atomic transport along shear bands is facilitated by excess volume re-distribution. In this respect the relaxation after deformation represents a localized "aging" effect. A phenomenological model of shear band initiation, evolution and relaxation is proposed. Generally, the current results point towards the importance of local stresses and non-affine deformation concerning glass relaxation and they also indicate clearly that local rearrangements induced by thermal attenuation or by deformation are not identical, rendering descriptions based on "effective temperature"- concepts inapplicable.

Acknowledgment

The financial support of the Deutsche Forschungsgemeinschaft (DFG) in the framework of SPP1594 – Topological Engineering of Ultra-Strong Glasses, Projects WI 1899/27-2 and HO 2231/8-2, is gratefully acknowledged. Technical support by Dr. Heiko Gerstenberg (TU Munich, Germany) in the ^{110m}Ag isotope production at the research reactor FRM II is appreciated. SD acknowledges the partial financial support of the Ministry of Education and Science of the Russian Federation in the framework of Increase Competitiveness Program of NUST «MISiS» (№ К3-2015-062).

References

[1] F. Spaepen, Microscopic mechanism for steady-state inhomogeneous flow in metallic glasses, Acta Metall. 25 (1977) 407–415.
[2] A. Argon, Plastic-deformation in metallic glasses, Acta Metall. 27 (1979) 47–58.
[3] C.A. Schuh, T.C. Hufnagel, U. Ramamurty, Overview No.144-mechanical behavior of amorphous alloys, Acta Mater 55 (2007) 4067–4109.

[4] A.L. Greer, Y.Q. Cheng, E. Ma, Shear bands in metallic glasses, Mater. Sci. Eng. R. 74 (2013) 71–132.
[5] M.L. Falk, J.S. Langer, Dynamics of viscoplastic deformation in amorphous solids, Phys. Rev. E 57 (1998) 7192–7205.
[6] J.-O. Krisponeit, S. Pitikaris, K.E. Avila, S. Küchemann, A. Krüger, K. Samwer, Crossover from random three-dimensional avalanches to correlated nano shear bands in metallic glasses, Nat. Commun. 5 (2014) 3616.
[7] Y. Shao, K. Yao, M. Li, X. Liu, Two-zone heterogeneous structure within shear bands of a bulk metallic glass, Appl. Phys. Lett. 103 (2013) 171901.
[8] J. Bokeloh, S.V. Divinski, G. Reglitz, G. Wilde, Accelerated diffusion along shear bands in metallic glass, Phys. Rev. Lett. 107 (2011) 235503.
[9] H. Rösner, M. Peterlechner, C. Kübel, V. Schmidt, G. Wilde, Density changes in shear bands of a metallic glass determined by correlative analytical transmission electron microscopy, Ultramicroscopy 142 (2014) 1–9.
[10] V. Schmidt, H. Rösner, M. Peterlechner, G. Wilde, P.M. Voyles, Quantitative measurement of density in a shear band of metallic glass monitored along its propagation direction, Phys. Rev. Lett. 115 (2015) 035501.
[11] J. Zausch, J. Horbach, The build-up and relaxation of stresses in a glass-forming soft-sphere mixture under shear: a computer simulation study, EPL 88 (2009) 60001.
[12] M. Ballauff, J.M. Brader, S.U. Egelhaaf, M. Fuchs, J. Horbach, N. Koumakis, M. Krüger, M. Laurati, K.J. Mutch, G. Petekidis, M. Siebenbürger, T. Voigtmann, J. Zausch, Residual stresses in glasses, Phys. Rev. Lett. 110 (2013) 215701.
[13] P. Chaudhuri, J. Horbach, Onset of flow in a confined colloidal glass under an imposed shear stress, Phys. Rev. E 88 (2013) 040301(R).
[14] P. Chaudhuri, J. Horbach, Poiseuille flow of soft glasses in narrow channels: from quiescence to steady state, Phys. Rev. E 90 (2014) 040301(R).
[15] W. Kob, H.C. Andersen, Kinetic lattice-gas model of cage effects in high-density liquids and a test of mode-coupling theory of the ideal-glass transition, Phys. Rev. E 48 (1993) 4364–4377.
[16] A.W. Lees, S.F. Edwards, Computer study of transport processes under extreme conditions, J. Phys. C. Solid State Phys. 5 (1972) 1921–1928.
[17] Y.P. Mitrofanov, M. Peterlechner, S.V. Divinski, G. Wilde, Impact of plastic deformation and shear band formation on the boson heat capacity peak of a bulk metallic glass, Phys. Rev. Lett. 112 (2014) 135901.
[18] G. Wilde, S.G. Klose, W. Soellner, G.P. Görler, K. Jeropoulos, R. Willnecker, H.J. Fecht, On the stability limits of the undercooled liquid state of Pd-Ni-P, Mater. Sci. Eng. A 226–228 (1997) 434.
[19] Yu.P. Mitrofanov, M. Peterlechner, I. Binkowski, M.Yu Zadorozhnyy, I.S. Golovin, S.V. Divinski, G. Wilde, The impact of elastic and plastic strain on relaxation and crystallization of Pd–Ni–P-based bulk metallic glasses, Acta Mater 90 (2015) 318–329.
[20] P.A. Duine, J. Sietsma, A. van den Beukel, Atomic transport in amorphous Pd40Ni40P20 near the glass-transition temperature – Au diffusivity and viscosity, Phys. Rev. B 48 (1993) 6957–6965.
[21] J. Ribbe, D. Baither, G. Schmitz, S.V. Divinski, Network of porosity formed in ultrafine-grained copper produced by qqual channel angular pressing, Phys. Rev. Lett. 102 (2009) 165501.
[22] G. Wilde, G.P. Görler, R. Willnecker, H.J. Fecht, Calorimetric, thermomechanical, and rheological characterizations of bulk glass-forming Pd40Ni40P20, J. Appl. Phys. 87 (2000) 1141–1152.
[23] G.P. Johari, Calorimetric features of release of plastic deformation induced internal stresses, and approach to equilibrium state on annealing of crystals and glasses, Thermochim. Acta 581 (2014) 14–25.
[24] S.V. Madge, D.T.L. Alexander, A.L. Greer, An EFTEM study of compositional variations in Mg-Ni-Nd bulk metallic glasses, J. Non Cryst. Solids 317 (2003) 23–29.
[25] G. Kumar, P. Neibecker, Y.H. Liu, J. Schroers, Critical fictive temperature for plasticity in metallic glasses, Nat. Commun. 4 (2013) 1536.
[26] T. Sentjabrskaja, P. Chaudhuri, M. Hermes, W.C.K. Poon, J. Horbach, S.U. Egelhaaf, M. Laurati, Creep and flow of glasses: strain response linked to the spatial distribution of dynamical heterogeneities, Sci. Rep. 5 (2015) 11884.
[27] G.P. Shrivastav, P. Chaudhuri, J. Horbach, Formation and growth of shear bands in glasses: existence of an underlying directed percolation transition, Prepr. arXiv:1506.03049 (2015).
[28] A. Paul, T. Laurila, V. Vuorinen, S.V. Divinski, Thermodynamics, Diffusion and the Kirkendall Effect in Solids, Springer Int. Publ., Switzerland, 2014, ISBN 978-3-319-07460-3.
[29] K.A. Dahmen, Y. Ben-Zion, J.T. Uhl, Micromechanical model for deformation in solids with universal predictions for stress-strain curves and slip avalanches, Phys. Rev. Lett. 102 (2009) 175501.
[30] C.H. Scholz, The Mechanics of Earthquakes and Faulting, Cambridge Univ. Press, New York, 2002.
[31] R. Maaß, K. Samwer, W. Arnold, C.A. Volkert, A single shear band in a metallic glass: local core and wide soft zone, Appl. Phys. Lett. 105 (2014) 171902.
[32] S.V. Madge, H. Rösner, G. Wilde, Transformations in supercooled Pd40.5Ni40.5P19, Scr. Mater 53 (2005) 1147–1151.
[33] E. Ma, Tuning order in disorder, Nat. Mater. 14 (2015) 547–552.
[34] J. Bünz, T. Brink, K. Tsuchiya, F. Meng, G. Wilde, K. Albe, Low temperature heat capacity of a severely deformed metallic glass, Phys. Rev. Lett. 112 (2014) 135501.
[35] W. Götze, L. Sjogren, Relaxation processes in supercooled liquids, Rep. Prog. Phys. 55 (1992), 241–376.
[36] C.A. Volkert, F. Spaepen, Crossover relaxation of the viscosity of pd40ni40p19si1 near the glass-transition, Acta Metall. 37 (1989) 1355–1362.
[37] A. van den Beukel, S. van der Zwaag, A.L. Mulder, A semi-quantitative description of the kinetics of structural relaxation in amorphous Fe40Ni40B20, Acta Metall. 32 (1984) 1895–1902.
[38] A.L. Greer, J.A. Leake, Structural relaxation and crossover effect in a metallic glass, J. Non Cryst. Solids 33 (1979) 291–297.
[39] S.V. Ketov, Y.H. Sun, S. Nachum, Z. Lu, A. Checchi, A.R. Beraldin, H.Y. Bai, W.H. Wang, D.V. Louzguine-Luzgin, M.A. Carpenter, A.L. Greer, Rejuvenation of metallic glasses by non-affine thermal strain, Nature 524 (2015) 200–206.
[40] Z. Evenson, B. Ruta, S. Hechler, M. Stolpe, E. Pineda, I. Gallino, R. Busch, X-ray photon correlation spectroscopy reveals intermittent aging dynamics in a metallic glass, Phys. Rev. Lett. 115 (2015) 175701.
[41] R. Maaß, P. Birckigt, C. Borchers, K. Samwer, C.A. Volkert, Long range stress fields and cavitation along a shear band in a metallic glass: the local origin of fracture, Acta Mater 98 (2015) 94–102.
[42] I. Binkowski, S. Schlottbom, J. Leuthold, S. Ostendorp, S.V. Divinski, G. Wilde, Sub-micron strain analysis of local stick-slip motion of individual shear bands in a bulk metallic glass, Appl. Phys. Lett. 107 (2015) 221902.
[43] F. Faupel, W. Frank, M.-P. Macht, H. Mehrer, V. Naundorf, K. Rätzke, H.R. Schober, S.K. Sharma, H. Teichler, Diffusion in metallic glasses and supercooled melts, Rev. Mod. Phys. 75 (2003) 237–280.
[44] V.N. Perevezentsev, A.S. Pupynin, Equations of diffusion in nonequilibrium grain boundaries, Phys. Met. Metall. 105 (2008) 322–326.
[45] S.V. Divinski, G. Reglitz, I. Golovin, M. Peterlechner, G. Wilde, Effect of heat treatment on diffusion, internal friction, microstructure and mechanical properties of ultrafine grained nickel severely deformed by equal channel angular pressing, Acta Mater 82 (2015) 11–21.
[46] N. Nollmann, I. Binkowski, V. Schmidt, H. Rösner, G. Wilde, Impact of micro-alloying on the plasticity of Pd-based bulk metallic glasses, Scr. Mater 111 (2015) 119–122.
[47] R.G. Faulkner, Nonequilibrium grain-boundary segregation in austenitic alloys, J. Mater. Sci. 16 (1981) 373–383.
[48] T.D. Xu, B.Y. Cheng, Kinetics of non-equilibrium grain-boundary segregation, Prog. Mater. Sci. 49 (2004) 109–208.